Research at the Fragment Mass Analyzer at ATLAS*

C. N. Davids,[a] B. Back,[a] I. G. Bearden,[b] K. Bindra,[a],[c] C. R. Bingham,[d] R. Broda,[b],[e] M. P. Carpenter,[a] W. Chung,[a],[f] L. Conticchio[g] P. J. Daly,[b] B. Fornal,[b] M. Freer,[a] Z. W. Grabowski,[b] D. J. Henderson,[a] R. G. Henry,[a] R. V. F. Janssens,[a] C.-L. Jiang,[a],[h] T. L. Khoo,[a] T. Lauritsen,[a] Y. Liang,[a] R. H. Mayer,[b] D. Nisius,[b] A. V. Ramayya,[c] F. Scarlassara,[i] F. Soramel,[a],[i] P. Spolaore,[i] W. B. Walters[g], A. H. Wuosmaa[a], and B. E. Zimmerman,[d]

[a]Argonne National Laboratory, Argonne, IL
[b]Purdue University, W. Lafayette, IN
[c]Vanderbilt University, Nashville, TN
[d]University of Tennessee, Knoxville, TN
[e]Institute of Nuclear Physics, Cracow, Poland
[f]University of Notre Dame, South Bend, IN
[g]University of Maryland, College Park, MD
[h]Institute of Atomic Energy, Beijing, People's Republic of China
[i]Legnaro National Laboratory, Legnaro, Italy

The experimental program at the Fragment Mass Analyzer (FMA) at the ATLAS accelerator is well under way. Experiments have been carried out at the target position and at the focal plane. After a brief facility description, some recent experimental results are presented.

1. Introduction

The FMA[1,2] is an 8.2-meter-long triple-focussing recoil mass spectrometer installed at the ATLAS heavy-ion accelerator at Argonne National Laboratory. Figure 1 shows a schematic diagram of the FMA.

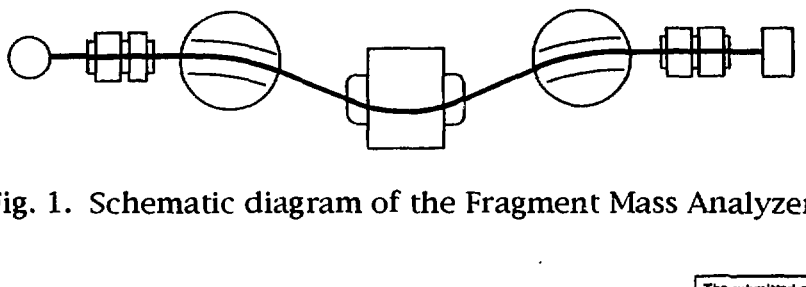

Fig. 1. Schematic diagram of the Fragment Mass Analyzer.

The FMA separates reaction products from the primary heavy-ion beam and disperses them by M/q at the focal plane. When the FMA is positioned at 0°, the primary beam is stopped on the anode of the first electric dipole, and the two electric dipoles plus the bending magnet constitute an energy-dispersionless mass spectrometer for the reaction products. The two magnetic quadrupole doublets provide geometric focussing and control of M/q dispersion at the focal plane. The FMA has an energy acceptance of ±20%, an M/q acceptance of ±4%, a maximum solid angle of 8 msr, variable mass dispersion, and an M/q resolution of >300:1. The FMA can be positioned at angles between -5° and +45°, as well as at distances from the target variable from 10 - 100 cm in order to accommodate large detector arrays at the target. Figure 2 shows a photograph of the FMA.

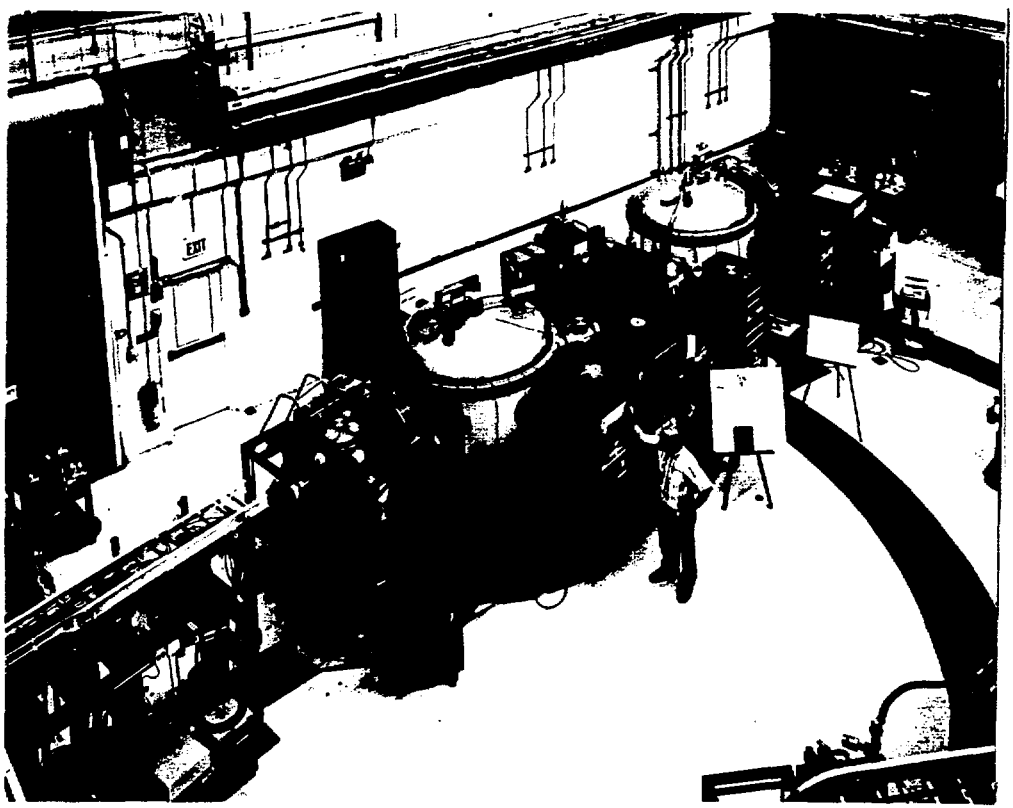

Fig. 2. Photograph of the FMA. The primary beam is incident from the lower left.

2. Experimental Equipment

A number of different experimental systems are available for use with the FMA. Some of these have been constructed by University users.

A 38-cm-diameter sliding-seal scattering chamber is available for use at the target position. It has provision for a target ladder as well as a rotating target wheel used under high beam current conditions. There are two independently controlled rings for mounting detectors, and one side of the chamber has a 30.5-cm by 30.5-cm opening to accommodate an extension for housing large gas detectors. All variable parameters are equipped with stepping motors, controlled manually or by computer. With this scattering chamber in place, the normal distance between the target and the entrance quadrupole is 30 cm. Vacuum is provided by a 1500 l/s cryopump attached to the side of the chamber.

For prompt gamma-ray experiments, an array of ten Compton-suppressed Ge detectors can be placed around the FMA target position. With these installed, the distance between the target and the FMA is 35.6 cm. For experiments with the Ge array, the 38-cm scattering chamber is replaced by a 12.1-cm-diameter target chamber containing a Si detector beam monitor, a target ladder driven by a stepping motor, and a device to insert thin carbon foils behind the target. These foils are used to reset the charge state of the reaction products following the emission of de-excitation gamma rays.

A 16-segment neutron detector array is available for use at the FMA target position, used in conjunction with the Compton-suppressed Ge detectors. It occupies the region between the small target chamber and the entrance to the FMA, so that neutrons evaporated in the forward direction can be detected. The detectors utilize pulse shape to discriminate between neutrons and gamma rays at neutron energies above 1 MeV, and time-of-flight for lower energies.

At the FMA focal plane a 15-cm horizontal by 5-cm vertical parallel-plate avalanche counter (PPAC) is used to measure x- and y-position, time, and energy loss. The PPAC has entrance and exit windows each of thickness 140 $\mu g/cm,^2$ and uses isobutane gas at a pressure of 3 Torr. Behind it can be placed other detectors such as Si or Bragg curve detectors, or the recoils can be allowed to proceed into other detector systems. A moving tape collector is available for measurement of beta activities, and a facility to study nuclear moments is under construction behind the FMA. It consists of a tilted foil array for polarizing the recoils,

and a magnet for beta-NMR measurements. Also available is an implantation-decay detection system using a 48 x 48 strip double-sided silicon strip detector.

3. Some Experimental Results

3.1 Yrast Isomers in ^{151}Yb

Reaction products have transit times through the FMA in the range 0.5-2 μs, providing an ideal opportunity to study the decays of microsecond isomers at the focal plane. In such an experiment,[3] the ^{96}Ru + 255 MeV ^{58}Ni reaction was used to produce fusion products near mass 151. After passing through the PPAC, the recoils were stopped on a catcher foil placed 10 cm behind the focal plane. Delayed gamma-recoil and gamma-gamma coincidences from the stopped

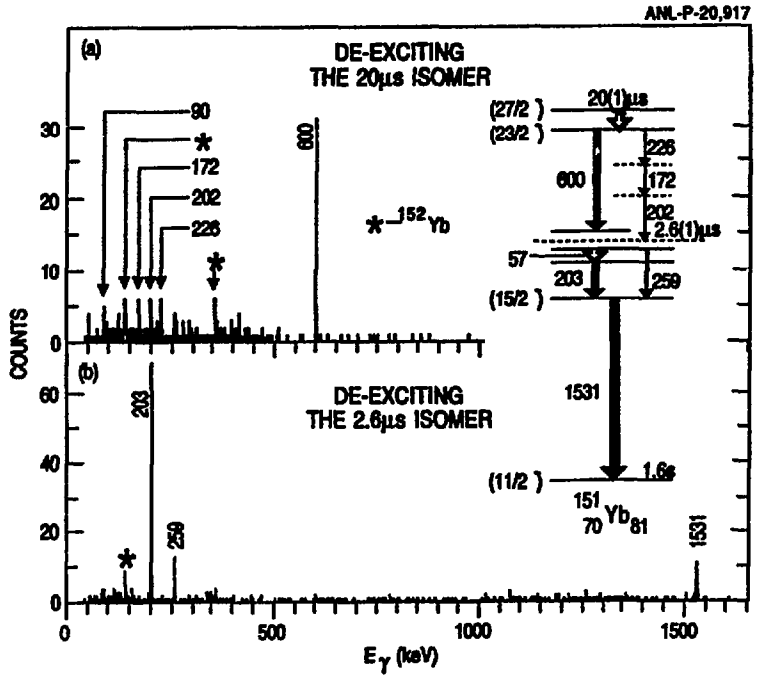

Fig. 3. Gamma rays observed at the FMA focal plane from the decay of high-spin isomers in ^{151}Yb.

recoils were measured between the PPAC and three gamma detectors. Besides transitions resulting from the decay of the known N = 82 isomers 2.6 μs ^{150}Er, 0.46 μs ^{151}Tm and 34 μs ^{152}Yb, two yrast isomers with half-lives of 20 ± 1 μs and 2.6 ± 0.7 μs were observed in ^{151}Yb. Figure 3 shows the clean separation of transitions feeding and de-exciting the 2.6 μs isomer, obtained by sorting the mass-selected gamma-gamma coincidence events using appropriate timing conditions. Further work on these isomers is planned, in particular the observation of conversion electrons using a Si detector.

3.2 Gamma Spectroscopy of Hg Isotopes

A number of gamma-ray spectroscopic studies using the array of ten Compton-suppressed Ge detectors around the FMA target position have been conducted. The reactions ^{155}Gd + ^{32}S (160 and190 MeV) and ^{160}Gd + ^{36}S (157 MeV) were used to produce $^{181\text{-}183}$Hg and $^{190\text{-}192}$Hg. The FMA transmissions obtained in these runs were 5-10%, with 2 charge states on the focal plane.

The data obtained from the ^{36}S + ^{160}Gd reaction demonstrate the sensitivity of the FMA for weak channels. Figure 4 shows how the mass resolution of the FMA allows one to pull out the gamma rays from the weakly-produced mass 189 channel for analysis of recoil-gamma-gamma coincidences.

3.3 Proton Radioactivity of ^{146,147}Tm

The ^{58}Ni + ^{92}Mo reaction was used to produce the isotopes ^{146}Tm and ^{147}Tm. Two different bombarding energies were used: 261 MeV to favor the production of ^{147}Tm, and 290 MeV to produce ^{146}Tm. ^{147}Tm is known to have two proton-emitting states, separated by about 60 keV.[4] Reaction products having a single M/q value were allowed to pass through the PPAC at the focal plane, and were implanted into a double-sided silicon strip detector (DSSD) located 27 cm behind the focal plane. The optics of the FMA produced a uniform illumination of the 1.6-cm x 1.6-cm DSSD, allowing it to serve as a 2304-pixel memory device. In this way, recoils were identified by PPAC-DSSD coincidences, and their locations and times of arrival were recorded. When a subsequent decay event occurred in that pixel, its time and energy was recorded. Data were recorded during a twenty-hour run with 2 particle nA of beam and an implantation count-rate of 60 Hz.

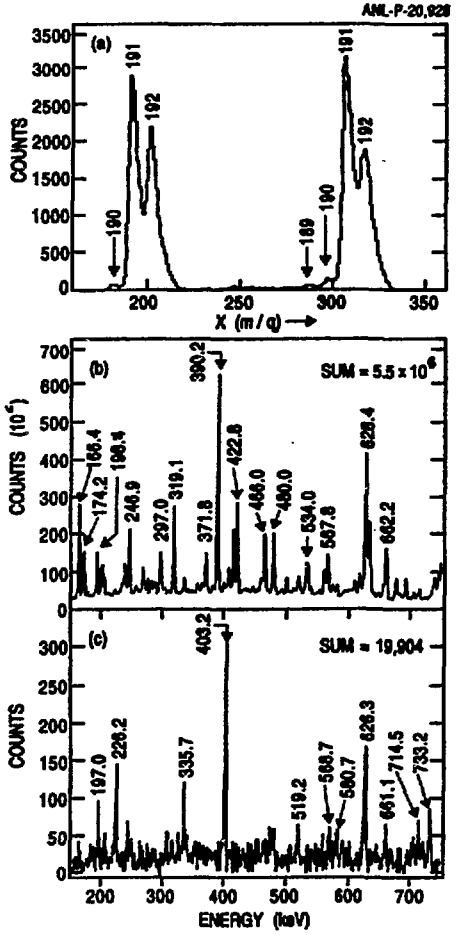

Fig. 4. Results from the $^{36}S + ^{160}Gd$ reaction. (a) Mass projection showing the low yield of mass 189. (b) A portion of the total γ-projection of the recoil-γ-γ matrix. Gamma rays from all masses observed in recoil coincidence are present, and the position of the strongest transition in ^{189}Hg at 403 keV is identified. (c) A portion of the mass 189-gated γ-projection of the recoil-γ-γ matrix.

Figure 5(a) shows the energy spectrum of decay events from mass 147 implants for implantation-decay time intervals between 10 ms and 5 s, while Figure 5(b) shows the same spectrum for time intervals less than 10 ms.

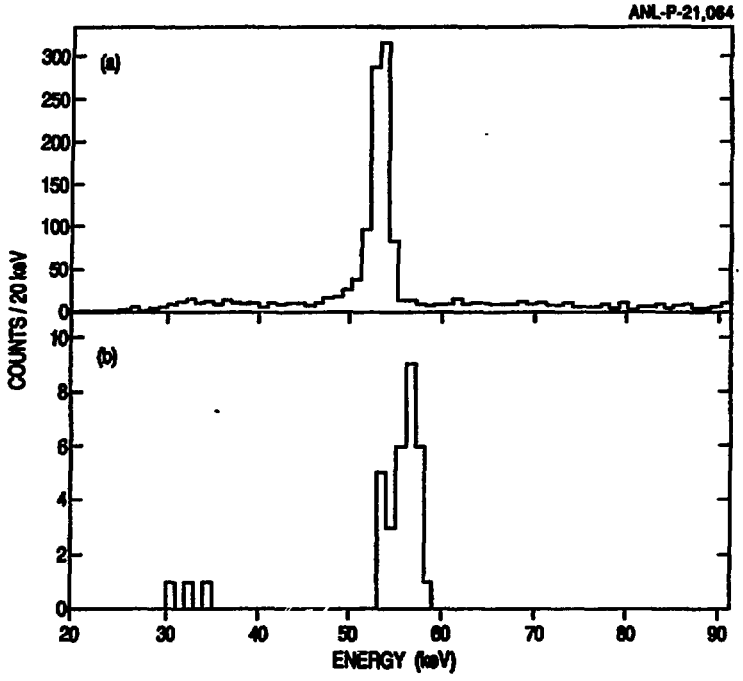

Fig. 5. Energy spectrum of decay protons implanted into a DSSD detector behind the FMA focal plane. (a) Implantation-decay-time intervals > 10 ms but < 5 s. (b) Implantation-decay-time intervals < 10 ms.

Using 740 events, the half-life of ^{147g}Tm was determined by least-squares fitting to be 559(26) ms, in excellent agreement with previous values.[4] The maximum likelihood method applied to 23 ^{147m}Tm decay events yielded a half-life of 390(+93-71) μs, also in excellent agreement with earlier work. Using 133 events, the half-life of ^{146g}Tm was determined by least-squares fitting to be 206(25) ms, in excellent agreement with work at Daresbury.[5] The maximum likelihood method applied to 15 ^{146m}Tm decay events yielded a half-life of 62(+19-14) ms, also in excellent agreement with earlier work.[5] Figure 6 shows the implantation-decay time interval spectra for ^{147g}Tm and ^{146g}Tm. In

future experiments the implantation system will be enlarged and used to search for new proton and alpha emitters.

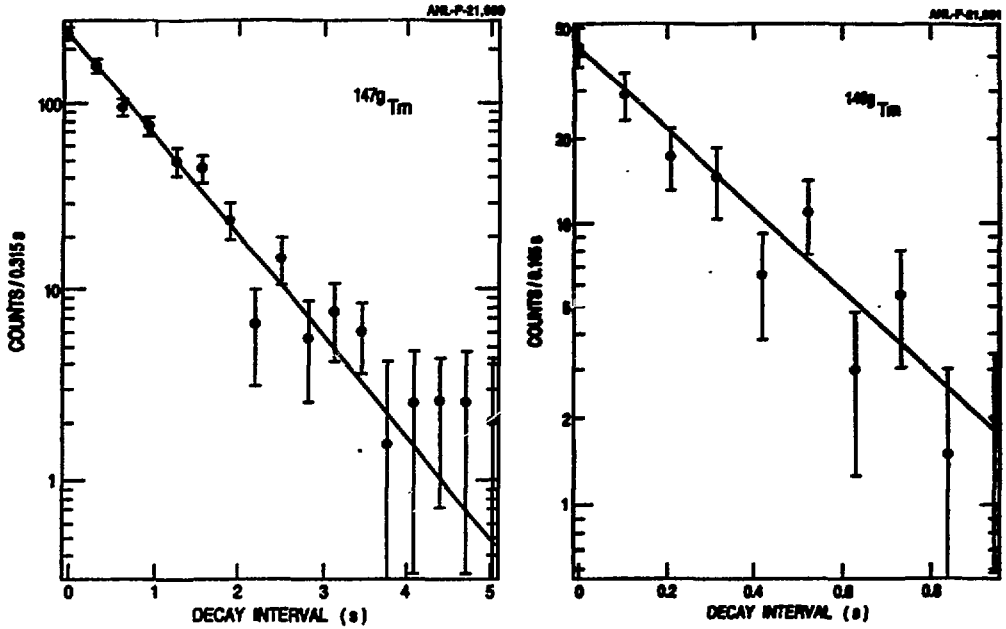

Fig. 6. Implantation-decay-time interval spectra for (a) ^{147g}Tm and (b) ^{146g}Tm. The solid lines are least-square fits.

4. Operational Properties of the FMA

The primary beam transmission of the FMA is defined as the intensity of primary beam particles measured on the focal-plane detector divided by the primary beam intensity at the target. The transmission has been measured using a ^{58}Ni beam on a number of targets with masses between 27 and 197. The values ranged from 10^{-6} in the former case to 10^{-11} for the latter. Low primary beam transmissions are obtained by using light beams and heavy targets.

The recoil transmission of the FMA is defined as the number of recoils reaching the focal plane divided by the number of recoils produced at the target, and is highly dependent on a number of variables. First is the FMA's geometric acceptance, typically 5 msr. The transmission also depends on the reaction kinematics and the target thickness, because

they determine the angular-, energy-, and charge-state distribution for recoils emerging from the target. Finally, the transmission depends on the M/q of the recoil compared to the central M/q. The transmission of a particular recoil species is measured by observing, in singles and in coincidence with recoils at the focal plane, a particular gamma transition at the target position. The highest transmission measured so far is from a ^{58}Ni on ^{64}Ni experiment. Here a transmission of 24% was measured for the 2p2n evaporation product ^{118}Xe. Figure 7 shows the M/q spectrum obtained during that measurement, showing two charge states for M = 118 on the focal plane.

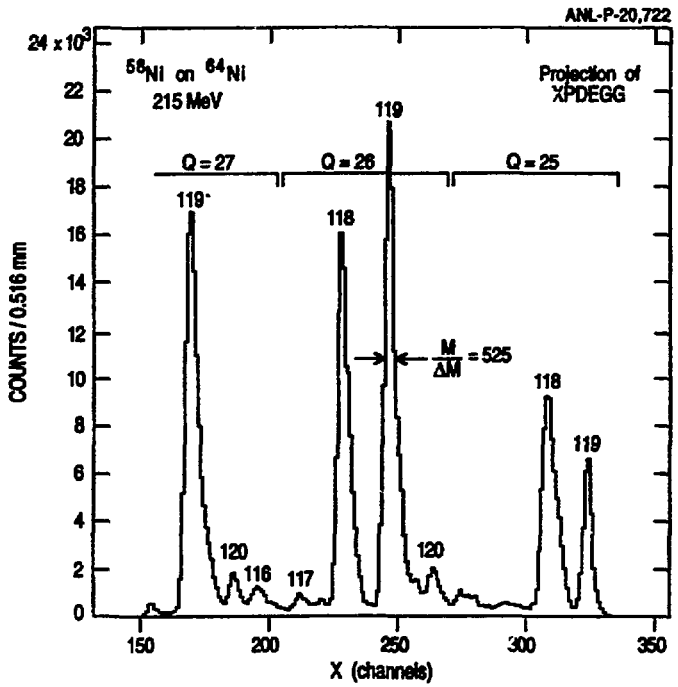

Fig. 7. M/q spectrum at the FMA focal plane from the ^{58}Ni + ^{64}Ni reaction at 215 MeV.

The mass resolution of the FMA is determined by the beam spot size on target and the angular and energy distributions of the recoils. A circular beam spot size of about 1-mm diameter is used at the FMA target. The highest mass resolution obtained so far with the FMA, 525:1, is shown in Figure 7. In other experiments where the reaction kinematics have been less favorable, mass resolutions of about 300:1 have been

obtained. Multiple scattering of the reaction products limits the target thicknesses to values typically between 300 and 700 μg/cm.[2]

The FMA has been tested with reactions utilizing both conventional and inverse kinematics. Inverse kinematics has the advantages of high transmission due to forward focussing of the recoils, and high recoil energies which aids in Z-identification. It has the disadvantages of worse primary beam attenuation and large gamma-ray Doppler shifts at the target.

At present, development work is proceeding on new configurations of detectors for the focal plane, including highly-segmented Si detectors for implantation studies and a gas ionization chamber for Z-identification.

References

*Work supported by the U.S. Department of Energy, Nuclear Physics Division, under contract W-31-109-ENG-38.

1. C. N. Davids and J. D. Larson, *Nucl. Instrum. and Methods* **B40/41**, 1224 (1989).
2. C. N. Davids *et al.*, *Nucl. Instrum. and Methods* **B70** 358 (1992).
3. D. Nisius *et al.*, *Phys. Rev.* C, May 1993.
4. S. Hofmann, in *Particle Emission from Nuclei Vol II*, ed. D. N. Poenaru and M. S. Ivascu, CRC Press (1989) Chapter 2.
5. K. Livingston *et al.*, *Phys. Lett. B*, accepted for publication (1993); P. J. Sellin *et al.*, *Phys. Rev. C*, May 1993.